Clinical and Translational Radiation Oncology 18 (2019) 131–139

Contents lists available at ScienceDirect

Clinical and Translational Radiation Oncology

journal homepage: www.elsevier.com/locate/ctro

Review Article

Repetitive MRI of organs at risk in head and neck cancer patients undergoing radiotherapy

Sonja Stieb [a,*], Baher Elgohari [a,b], Clifton David Fuller [a]

[a] Department of Radiation Oncology, The University of Texas MD Anderson Cancer Center, Houston, TX, USA
[b] Department of Clinical Oncology and Nuclear Medicine, Mansoura University, Mansoura, Egypt

ARTICLE INFO

Article history:
Received 1 April 2019
Revised 16 April 2019
Accepted 16 April 2019
Available online 26 April 2019

Keywords:
Radiotherapy
Head and neck cancer
Repetitive MRI
Imaging biomarker

ABSTRACT

With emerging technical advances like real-time MR imaging during radiotherapy (RT) with an integrated MR linear accelerator, it will soon be possible to analyze changes in the organs at risk (OARs) during radiotherapy without additional effort for the patients. Until then, patients have to undergo additional MR imaging and often without the same immobilization devices as used for radiotherapy. Consequently, studies with repetitive MRI during the course of radiotherapy are rare, with low patient numbers and with the challenge of registration between the different MR sequences and the varying imaging time points.

This review focuses on studies with at least two MRIs, one before and another either during or post-RT, in order to report on RT-induced changes in normal tissues and their correlation with toxicity. We therefore included clinical studies published in English until March 2019, with repetitive MRI of OARs in head and neck cancer patients receiving external beam radiotherapy. OARs analyzed were salivary glands, musculoskeletal structures and bones. MR sequences used included T1, T2, dynamic contrast enhanced (DCE) imaging, diffusion-weighted imaging (DWI), DIXON and MR sialography.

Contents

* Corresponding author at: Department of Radiation Oncology, The University of Texas MD Anderson Cancer Center, 1515 Holcombe Blvd, Houston, TX 77030, USA.
E-mail address: smstieb@mdanderson.org (S. Stieb).

https://doi.org/10.1016/j.ctro.2019.04.014
2405-6308/

1. Introduction

The standard of care in locally advanced head and neck cancer is combined chemoradiation. Even in very advanced stages, especially for human papilloma virus (HPV) associated oropharyngeal cancer (OPC) patients, the loco-regional control rates are promising with 85% still alive after a follow-up of five years from chemoradiation [1]. These extraordinary high control rates led to an adaption of the AJCC staging system in 2018 including the HPV status in the tumor classification [2], and to even more approaches to de-intensify therapy in these patients [3].

With conventional radiation doses of up to 70 Gy using normal fractionation, the severe radiation-induced side effects are high for both, acute and late toxicities. In a recent large multicenter study published by Gillison et al. in 2019, the toxicity rates for OPC patients were reported as high as 50% and 32% for acute and late G2-3 xerostomia, 37% and 4% for acute and late G3-4 dysphagia and 42% for G3-4 acute mucositis [1]. Other, less common or less severe radiation-induced toxicities in head and neck cancer patients include taste changes [4], voice alteration [5] and osteoradionecrosis [6].

With emerging technical advances and the broad availability of MRI, a lot of effort has already been undertaken to identify functional MR imaging biomarkers for outcome and toxicity prediction. Most of the studies so far focused on MR changes in tumor tissue (Review: [7]) in order to adapt the treatment, i.e. by dose escalation or de-escalation. Although a de-intensified therapy will in most cases lead to reduced toxicity as well, additional research is necessary, to identify normal tissue biomarkers which serve as early predictors for acute and late toxicity by providing anatomical and functional information about size, cellularity, fibrosis, etc..

In this review we therefore focus on studies describing radiation-induced MRI changes across different sequences in OARs of the head and neck region before, during and after radiotherapy (RT).

2. Materials and methods

2.1. Literature search

A PubMed literature search has been independently conducted in March 2019 by two board-certified radiation oncologists (S.S.; B. E.). Studies have been included into this review, if the following criteria were met: 1.) Clinical studies published in English language, no case reports, no conference abstracts; 2.) Patients with head and neck cancer of the oral cavity, naso-, oro-, hypopharynx and larynx receiving external beam radiotherapy; 3.) MRI has been performed before radiotherapy and again during or post-RT; 4.) Analysis of MR changes in normal tissue.

2.2. Included studies

Twenty-one clinical studies, published between 2007 and 2018, have been extracted meeting the above mentioned inclusion criteria (Table 1). Of these studies, 16 analyzed MR changes in the salivary glands, three in musculoskeletal tissue and two in bony structures.

Nine studies included NPC patients only, five exclusively OPC patients and the remaining seven studies included patients with different head and neck tumor locations. MRI was performed on a 1.5 or 3.0 Tesla machine including sequences like T1, T2, T1 post contrast, dynamic contrast enhanced (DCE) imaging, diffusion-weighted imaging (DWI), intravoxel incoherent motion (IVIM) imaging, DIXON and MR sialography. The majority of studies assessed the MR changes before and post-RT, but at least nine studies also included a mid-therapy assessment.

3. Results and discussion

3.1. Quantitative changes in MRI of the salivary glands

Of the 16 studies analyzing MR changes during the course of radiotherapy in the salivary glands, all included the parotid glands (PG) and eight studies additionally the submandibular glands (SMG). No study so far included the sublingual glands. All patients in these studies received primary or postoperative, curatively-intended, radio(chemo)therapy with IMRT [8–24,26–28] or 3D-radiotherapy [25,27,28]. Radiation doses to the primary tumor ranged from 60 to 74 Gy. Chemotherapy was mainly concurrent and platinum-based, but also induction or adjuvant chemotherapy has been prescribed.

MRI during radiotherapy was performed between week 2 and 5, and post-treatment MRI from end of treatment until 16 months post-RT.

3.1.1. T1/T2 (Table 2)

T1 weighted signal intensity (SI) (“spin-lattice”), accounting for the tissue-dependent longitudinal relaxation time following a radiofrequency pulse, was reported to significantly decrease by 8% and 11% in the parotid and submandibular glands from baseline to six weeks after end of radiotherapy, respectively, measured with a spin echo sequence [23].

The T1rho value, also known as “spin lock” combining aspects of T1 and T2 weighted imaging, significantly increased in the parotid gland during radiotherapy showing higher values at mid-treatment and even higher values at post-treatment, but no significant correlation could be shown with xerostomia or dose [12].

The T2 weighted SI (“spin-spin”), measuring the transverse relaxation, increased until week 5 of radiotherapy by 6% and further increased until 4 weeks from end of treatment by additional 5%, resulting in a total change of 11%, measured by Zhou et al. [9]. Houweling et al. found a similar increase in T2 SI for the parotid glands with values of +13%, and a higher increase of +29% for the submandibular glands 6 weeks post-RT [23]. The same increase in T2 SI as for the submandibular glands was reported for the high-dose areas only of both salivary glands, which was defined as mean dose of >30 Gy for the parotid glands and >49 Gy for the submandibular glands [23].

Table 1
Overview of clinical studies in head and neck cancer patients with MRI before radiotherapy (pre) and at least one additional MR measurement during (mid) or post-radiotherapy (post).

Author, year	Tumor localization	N	T	MR Sequence	OAR	MRI		
						pre	mid	post
Marzi, 2018 [8]	OP	40	1.5	IVIM, DCE	SG	x	x	x
Zhou, 2018 [9]	NP	28 (19)*	3.0	T2mapping, mDIXON Quant	SG	x	x	x
Zhang, 2018 [10]	NP	26	3.0	DWI	SG	x	x	x
Meheissen, 2018 [11]	OP	46	3.0	T1, T2, T1c	MS	x	x	x
Zhou, 2017 [12]	NP	26	3.0	T1rho	SG	x	x	x
Loimu, 2017 [13]	OP, L	20	1.5	DWI	SG	x		x
Hatakeyama, 2017 [14]	OP	39	1.5/3.0	T1, T2	Bone	x		x
Messer, 2016 [15]	NP	72	1.5	T1, T2	MS	x		x
Sandulache, 2016 [16]	OP	32	3.0	DCE	Bone	x	x	x
Marzi, 2015 [17]	OP, NP, HP, L	34	1.5	IVIM	SG	x	x	x
Juan, 2015 [18]	NP	11	1.5	DWI	SG	x		x
Doornaert, 2014 [19]	OP, HP	8	1.5	DWI	SG	x	x	x
Zhang, 2013 [20]	NP	28	3.0	DWI	SG			
Ou, 2013 [21]	NP	14	3.0	MR sialography	SG	x		x
Cheng, 2013 [22]	NP	16	1.5	DCE	SG	x		x
Houweling, 2011 [23]	OP	18	3.0	T1, T2, DCE	SG	x		x
Lee, 2011 [24]	NP	21	1.5	DCE	SG	x		x
Kan, 2010 [25]	OP, NP, HP, L, PS, UP	14	1.5	T2	SG	x	x	x
Popovtzer, 2009 [26]	OP, NP, HP, UP	12	3.0	T1, T2	MS	x		x
Dirix, 2008 [27]	OP, OC, UP	8	1.5	DWI	SG	x		x
Astreinidou, 2007 [28]	OP, NP	9	1.5	MR sialography	SG	x	(x)	(x)

* 28 patients with repetitive T2, 18 patients with repetitive DIXON. DCE: dynamic contrast enhanced imaging, DWI: diffusion weighted imaging, HP: hypopharynx, IVIM: intravoxel incoherent motion imaging, L: larynx, MS: musculoskeletal, NP: nasopharynx, OAR: organ at risk, OC: oral cavity, OP: oropharynx, PS: paranasal sinus, SG: salivary gland, T: magnetic field strength in Tesla, T1c: T1 post contrast, UP: unknown primary.

Table 2
Changes in T1/T2 MRI of salivary glands during the course of radiotherapy.

Author, year	OAR	Timepoint	Main findings
Zhou, 2018 [9]	PG	BL 5w after RT-start 4w post-RT	T2 values sign. Increase from BL to mid-RT (+6%) and post-RT (+11%). No sign. correlation between dT2 and mean RT dose.
Zhou, 2017 [12]	PG	BL 5w after RT-start 4w post-RT	T1rho sign. increases from BL to mid-RT (+21%) and post-RT (+29%), No sign. correlation of change in T1rho with dose or xerostomia.
Houweling, 2011 [23]	PG, SMG	BL 6w post-RT	Sign increase post-RT in T2 SI (+13%/+29%) and sign. decrease in T1 SI (−8%/−11%) in both SG. Sign. Correlation between change in T2 SI and dose.

BL: baseline, OAR: organ at risk, PG: parotid gland, RT: radiotherapy, SG: salivary gland, SI: signal intensity, sign.: significant/ly, SIR: signal intensity ratio, SMG: submandibular gland, w: week.

Table 3
Changes in DCE MRI of salivary glands during the course of radiotherapy.

Author, year	OAR	Time point	Main findings
Cheng, 2013 [22]	PG	BL Mean 53d post-RT	Post-RT, PGs showed a sign. higher A (+87%), peak enhancement (+93%, in all patients higher than BL values), wash-in slope (+73%) and a sign. lower K_{el} (−57%). No sign. change in k_{21} and TTP. Only peak enhancement with sign. positive correlation to dose. K_{el} and slope with sign. negative and TTP with sign. positive correlation to PSV.
Houweling, 2011 [23]	PG, SMG	BL 6w post-RT	Sign increase post-RT in v_e (+33%/+23%) and sign. decrease in k_{ep} (−16%/−24%) in PGs and SMGs, respectively. No sign. difference from BL to post-RT in k_{trans} and v_p.
Lee, 2011 [24]	PG	BL 3 m post-RT	Sign. increase in k_{trans} (+71%), v_e (+93%), v_p (+477%) post-RT.

BL: baseline, k_{21}: contrast exchange rate constant, k_{el}: elimination transfer rate, k_{ep}: flux rate constant, k_{trans}: volume transfer coefficient, m: month, OAR: organ at risk, PG: parotid gland, PSV: parotid sparing volume, defined as percentage of PG receiving < 25 Gy, RT: radiotherapy, sign.: significant, SMG: submandibular gland, TTP: time-to-peak, v_e: extravascular volume fraction, v_p: vascular plasma space, w: week.

Contradicting results are reported for the correlation between T2 SI and dose: Houweling et al. found a significant association between these parameters [23], whereas Zhou et al., including 1.5 times more patients than Houweling, did not [9].

3.1.2. DCE (Table 3)

DCE imaging provides pharmacokinetic perfusion parameters after injection of intravascular contrast medium, like the volume transfer coefficient k_{trans}, the flux rate constant k_{ep}, the vascular

Table 4
Changes in DWI/IVIM parameters during and after radiotherapy compared to baseline values in salivary glands.

Author, year	OAR	Time point	Main findings
Zhang, 2018 [10]	PG, SMG	BL 2w after RT-start	ADC sign. increased during RT in both, PGs (median ADC +44%) and SMGs (+27%). ADC sign. decreased during RT in the PGs (−25%) and non-significantly in the SMGs (-13%), same for the difference between ADC after stimulation and ADC at rest (PGs: −42%, sign., SMGs: −24%, n.s.). ΔADC at rest and after stimulation of the PGs sign. correlated with degree of xerostomia 6 months post-RT (r = 0.41/−0.61/−0.72), whereas ΔADC of the SMGs did not.
Loimu, 2017 [13]	PG, SMG	BL 6m post-RT	PGs with sign. higher ADC values than SMGs. ADC sign. increased from BL to post-RT for both, PGs (+29%) and SMGs (+28%). ADC after stimulation sign. higher post-RT than at BL. Sign. linear correlation between change of ADC from BL to post-RT with dose for both, PGs and SMGs.
Marzi, 2015 [17]	PG	BL fx16-17 Last fx	Sign. increase in all diffusion parameters, ADC (+15%/+21%), ADC_{low}, D and f, from baseline to mid- and post-treatment, respectively. D only diffusion parameter with sign. correlation to PG dose.
Juan, 2015 [18]	PG	BL Mean 7w post-RT Mean 8m post-RT Mean 16m post-RT	ADC increased by 36% (post-RT TP 1, sign.), 27% (post-RT TP 2, sign.) and 20% (post-RT TP 3, sign.). ADC with sign. neg. correlation to PG volume and sign. pos. correlation to dose. Patients with G1/2 xerostomia with sign. higher ADC.
Doornaert, 2014 [19]	PG, SMG	BL, 20–22 Gy, 2–3 m post-RT	SMGs with higher ADC values than PGs. Increase in ADC from BL to mid-RT (EPI DWI: +18%/HASTE DWI: 9%) and further increase to post-RT (+39%/+44%).
Zhang, 2013 [20]	PG	BL Within 2w post-RT	ADC (+44%) and increase of ADC after stimulation sign. increased post-RT.
Dirix, 2008 [27]	PG, SMG	BL Mean 9m post-RT	PGs with sign. higher ADC values than SMGs. Ipsilateral PGs with sign. increased ADC and no response to stimulation post-RT compared to BL. Contralateral PGs with no sign. change in ADC from BL to post-RT and similar response to stimulation (initial decrease followed by increase) post-RT. Both SGs with sign. increase of ADC post-RT, but only contralateral SGs with similar response to stimulation compared to BL.

ADC: apparent diffusion coefficient, ADC_{low}: ADC derived by low b-values, BL: baseline, D: true diffusion, EPI: echo planar imaging, f: perfusion fraction, HASTE: half-fourier acquisition single-shot turno spin-echo, m: months, n.s.: not significant, OAR: organ at risk, PG: parotid gland, RT: radiotherapy, SG: salivary gland, sign.: significant/ly, SMG: submandibular gland, TP: time point, w: week.

Table 5
Changes in mDIXON Quant of the salivary glands during the course of radiotherapy.

Author, year	OAR	Time point	Main findings
Zhou, 2018 [9]	PG	BL 5w after RT-start 4w post-RT	FF sign. increased from BL (38%) to mid-RT (42%, +9%) and then sign. decreased from mid- to post-RT (39%, −10%). No sign. correlation between ΔFF and mean RT dose.

BL: baseline, FF: fat fraction, OAR: organ at risk, PG: parotid gland, RT: radiotherapy, sign.: significant/ly, w: week.

plasma space v_p, the extravascular volume fraction v_e and the elimination transfer rate k_{el}.

From pre- to post-RT, a significant increase in v_e of 33% [23] to 93% [24] was reported for the parotid glands and of 23% for the submandibular glands [23]. V_e increased by 33% in salivary glands receiving low doses (mean dose PGs < 30 Gy, SMGs < 49 Gy) and by 40% in case of higher mean doses [23]. A significant increase after radiotherapy was also found for peak enhancement, which also correlated with dose, A (concentration-time curve amplitude) and wash-in slope [22]. A significant decrease post-treatment was shown for k_{ep} and was calculated as −16% for parotid and −24% for submandibular glands [23]. However, contradicting results between different studies [23,24] and for parotid versus submandibular glands [23] have been reported for k_{trans} and v_p. No significant change could be found for k_{21} (contrast exchange rate constant) and time-to-peak from baseline to post-RT [22].

3.1.3. DWI/IVIM (Table 4)

DWI describes the molecular diffusion, mainly of water, by providing the apparent diffusion coefficient (ADC). In case of IVIM, the

Table 6
Findings in MR sialography before, during and after radiotherapy of the head and neck region.

Author, year	OAR	Time point	Main findings
Ou, 2013 [21]	PG, SMG	BL 1w post-RT 1y post-RT	PG duct visibility at rest and after stimulation decreased to 65% 1 week post-RT and then increased to 96% (rest) and 100% (stimulated) 1 year post-RT. SMG duct visibility continued to decrease 1 year post-RT or remained stable (visibility 60% 1y post-RT), with no response to stimulation. Patients with G1 xerostomia showed a sign. higher PG duct visibility (duct score at rest 101%) 1 year post-RT compared to patients with G2 xerostomia (78%).
Kan, 2010 [25]	PG	BL, Mean 40d after RT-start (15-72d)	Main excretory duct width sign. decreased from 0.20 mm pre-RT to 0.15 mm 15–72 days after start of RT. Also decrease in main duct contrast and duct branch visibility (sign.)
Astreinidou, 2007 [28]	PG, SMG	BL 6w post-RT 6m post-RT	Average Stensen's duct width was 2.1 mm pre-RT and then increased to 2.2 mm and 2.3 mm 6 weeks and 6 months post-RT, respectively. The average SMG duct first decreased from 2.2 mm at BL to 2.0 mm post-RT and then slightly increased to 2.1 mm. Duct visibility decreased post-RT in PGs receiving mean doses >20 Gy and nearly all SMGs.

BL: baseline, d: days, G: grade, m: month, OAR: organ at risk, PG: parotid gland, RT: radiotherapy, sign.: significant/ly, SMG: submandibular gland, w: week, y: year.

true diffusion D can be determined with the use of more b-values for image acquisition, by subtracting the perfusion component, calculated with a specific formula including the signal intensity, (perfusion-related) pseudo-diffusion D* and perfusion fraction f.

At baseline, the ADC value in the parotid glands was significantly higher than in submandibular glands in two studies [13,27], but significantly lower in another study [19].

Consistently, a significant ADC increase was reported from pre- to mid- and post-RT in both glands. Compared to baseline values, the ADC of the parotid gland thereby increased by 15–44% during radiotherapy [10,17] and 21–41% 0–6 months post-RT [13,17,18,20] and then slowly decreased again until 16 months from radiotherapy (+20% from baseline) [18]. The ADC of the submandibular gland increased by 27% during [10] and 28% [13] post-treatment. If analyzed separately for ipsi- and contralateral salivary glands, the parotid glands showed a significant ADC increase of 29% only ipsilateral, whereas the submandibular gland showed a significant increase on both sides [27]. Similarly, ADC values derived from low b-values, D and f showed a significant increase post-RT [17].

After stimulation, ADC in both glands was reported to first increase and then decrease or fluctuate in three studies [10,13,20], whereas another group showed the opposite with initial decrease followed by an increase in ADC [27]. Contradicting results were also reported for the difference between maximum ADC after stimulation and ADC at rest in the parotid gland: Zhang et al. described a significant lower difference 2 weeks after start of radiotherapy than at baseline [10], Dirix et al. found no response at all in the ipsilateral gland post-RT [27], but Loimu et al. and Zhang et al. could show significant higher values after end of radiotherapy compared to baseline [13,20]. No significant change in ADC after stimulation was reported for the submandibular glands [10].

ADC at mid- and post-treatment compared to baseline values was significantly higher in patients with xerostomia [10,18], whereas the increase of ADC after stimulation showed a significant negative correlation [10]. The ADC of the submandibular glands did not correlate with xerostomia [10].

Regarding dose, there was a significant correlation with ADC in unstimulated and [13,18,19] stimulated condition [13], mid [19] and post-RT [13,18,19], reported in various studies.

3.1.4. DIXON (Table 5)

For mDIXON Quant imaging, a method to quantitatively assess the amount of fat by accounting for in-phase water, no significant correlation was found between radiation dose and fat fraction changes of the parotid glands. However, an increase of fat fraction was observed by mid therapy, but then returned to baseline values 4 weeks post-RT. Further studies are needed to investigate Dixon sequences as a predictive/prognostic biomarker.

3.1.5. Sialography (Table 6)

Several months after end of radiotherapy, the visibility of the salivary gland ducts is still significantly decreased in the MR sialography, acquired as heavily T2 weighted sequence with fat suppression [21,25,28]. However, after one year from radiotherapy, a nearly full recovery was detected for the parotid glands, whereas the visibility of the submandibular gland ducts further decreased or stayed at a lower level [21].

In concordance with the decrease in duct visibility, Kan et al. found a decrease in duct size from 0.20 mm before radiotherapy to 0.15 mm after 15–72 days from start of radiotherapy [25]. On the other side, Astreinidou et al. found a slight increase in size for the Stensen's ducts post-RT, although as well reporting a decreased duct visibility for glands receiving >20 Gy mean dose [28].

Duct visibility was significantly correlated with the grade of xerostomia post-RT [21].

3.1.6. Volume (Table 7)

With increasing doses through the course of radiotherapy, the salivary glands show a decrease in volume, measured on T1 and T2 MRI. At baseline, the parotid glands measured on average 25.7–32.3 cm^3, until the 10th fraction the volume already decreased by 18% [8] and until the fifth week of radiotherapy by 26–27% [9,12]. Then, the size of the parotid gland seems to remain relatively stable between −26 – −31% of the baseline value, measured at different time-points between the last fraction of radiotherapy and 8 months post-treatment within different studies (Table 7). Interestingly, the parotid gland increased in size again afterwards, but with −17% at 16 months post-RT remained below baseline values [18]. The submandibular gland showed a similar radiation-induced shrinkage as the parotid glands with 23% volume loss six weeks after end of radiotherapy [23]. However, no volumetric measurement during the course of radiotherapy was performed for the submandibular glands so far.

For the parotid gland, a significant correlation between the volumetric change during radiotherapy and baseline k_{ep}, as well as mid-RT $D_t/\Delta D_t$, ΔADC, Δf [8] and T1rho SI [12] has been reported. Also, a significant correlation with clinical and treatment parameters was found like baseline parotid gland volume, weight, BMI, dose and V30, however no correlation was found with weight loss during therapy [8]. The post-treatment shrinkage was significantly correlated with baseline k_{trans}, k_{ep}, IAUGC [8], ADC [18], v_e and v_p [24], as well as with $D_t/\Delta D_t$, f/Δf during RT [8] and ΔT2 SI [29] and v_e post-RT [24]. No correlation between parotid gland volume loss post-treatment and dose was found [8,18], however a significant association was reported with G1 and G2 xerostomia [18].

3.1.7. Summary

Although most of the studies analyzing changes in MRI of the OAR in the head and neck region focused on the salivary glands, in many cases there is still evidence from only one study available for some parameters. Furthermore it has to be considered that the studies included only up to 40 patients, so the results should be interpreted with caution. Keeping that in mind, the studies showed a radiation-induced increase in T1/T2 SI, T1rho, v_e, peak enhancement, A, wash-in-slope, ADC, D, f and fat fraction of the salivary glands. A decrease was reported for k_{ep}, duct visibility and volume. A correlation with xerostomia seems to exist for ADC, duct visibility and salivary gland volume.

3.2. Quantitative MRI changes in musculoskeletal structures of the head and neck region (Table 8)

To date, only one clinical study investigated the effect of radiotherapy on the muscles of the head and neck region during the course of treatment using MRI (Table 8).

Meheissen et al. included 46 OPC patients receiving 70 Gy radiotherapy concurrent with chemotherapy and conducted serial MR measurements before, during (week 3–4) and 6–8 weeks post-treatment [11]. They included 12 different swallowing muscles and used T1, T2 and T1 post contrast images for analysis.

Two other studies by Messer et al. and Popovtzer et al. analyzed the effect of radiochemotherapy on the swallowing muscles as well, but by using measurements before and after radiotherapy only [15,26](Table 8). Messer et al. included 72 NPC patients and conducted the T1 and T2 MRI before and after a median of 4 and 41 months, respectively [15]. They focused on the superior pharyngeal constrictor and the soft palate. Popovtzer et al. only included 12 patients with different tumor sites in the head and neck region and scanned the patients with T1 and T2 sequences before and

Table 7
Radiation-induced volumetric changes of the salivary glands.

Author, year	OAR	Time point	Main findings
Marzi, 2018 [8]	PG	BL fx10 w8 post-RT	PG volume decreased from BL (32.3 cm^3) to fx10 (26.7 cm^3, −18%) and further on until 8 weeks post-RT (22.7 cm^3, overall change from BL −31%). PG shrinkage during RT sign. correlated with BL k_{ep} and fx10 D_t, ΔADC, ΔD_t. Post-RT PG shrinkage sign. correlated with BL k_{trans}, k_{ep}, IAUGC and fx10 D_t, ΔD_t, f, Δf. Sign. association of PG shrinkage with BL PG volume, weight, BMI, dose and V30, but only at fx10. No correlation with general weight loss.
Zhou, 2018 [9]	PG	BL 5w after RT-start 4w post-RT	PG volume sign. decreased from BL (27.2 cm^3) to mid-RT (19.4 cm^3, −27%) and did not change from mid- to post-treatment (19.5 cm^3, overall change from BL −27%). Sign. correlation between ΔT2 and ΔPG volume pre- to post-RT.
Zhou, 2017 [12]	PG	BL 5w after RT-start 4w post-RT	PG volume sign. decreased from BL (25.7 cm^3) to mid-RT (18.9 cm^3, −26%) and did not change from mid- to post-treatment (18.3 cm^3, overall change from BL −29%). Sign. pos. correlation between change in PG volume and T1rho only mid-RT.
Marzi, 2015 [17]	PG	BL fx16-17 Last fx	PG volume decreased from BL (27.4 cm^3) to end of RT (19.5 cm^3, −31%). BL f and PG dose best independent predictors for PG shrinkage.
Juan, 2015 [18]	PG	BL Mean 7w post-RT Mean 8m post-RT Mean 16m post-RT	PG volume decreased from BL (26.2 cm^3) by −31% (post-RT TP1, sign.), − 26% (post-RT TP2, sign.) and −17% (post-RT TP3, n.s.). PG volume with sign. negative correlation to ADC. Patients with G1/2 xerostomia with sign. smaller PG volume. No sign. correlation between PG volume and dose.
Houweling, 2011 [23]	PG, SMG	BL 6w post-RT	PG and SMG volume both decreased from BL (29.4 cm^3/8.4 cm^3) to post-RT (21.7 cm^3, −26%/8.4 cm^3, − 23%).
Lee, 2011 [24]	PG	BL 3m post-RT	PG volume decreased by 32%. PG shrinkage sign. correlated with BL v_e, BL v_p and post-RT v_e

ADC: apparent diffusion coefficient, BL: baseline, BMI: body mass index, D_t: tissue diffusion coefficient, f: perfusion fraction, fx: fraction, G: grade, IAUGG: initial area under gadolinium concentration curve, k_{ep}: flux rate constant, k_{trans}: volume transfer coefficient, m: month, n.s.: not significant, OAR: organ at risk, PG: parotid gland, SMG: submandibular gland, sign.: significant/ly, TP: time point, V30: percentage of parotid gland volume receiving a dose ≥30 Gy, v_e: extravascular volume fraction, v_p: vascular plasma space, w: week

Table 8
Radiation-induced changes in T1, T2 and T1 post contrast in head and neck muscles.

Author, year	OAR	Time point	Main findings
Meheissen, 2018 [11]	Swallowing muscles	BL w3-4 after RT-start 6-8w post-RT	Sign. increase in T2 SI mid- and post-RT only in MPC. No sign. change in T1 for any muscle over time. Sign. increase in T1c SI mid- and post-RT in SPC and MPC and post-RT only in MP, MM, MH, GG, ITM, ADM, PDM. Percentage change of T2 and T1c SI mid- and post-RT sign. correlated with dose for all muscles analyzed together, but no correlation with T1 SI change. Patients developing moderate to severe dysphagia revealed higher T2 SI changes mid-RT and higher T1 SI changes post-RT.
Messer, 2016 [15]	SPC, soft palate	BL Median 4m post-RT Median 41m post-RT	SPC with mean doses ≥62.25 Gy revealed a sign. decrease in T1 SI late post-RT compared to BL. T2 SI sign. increased early after RT in SPC and soft palate and then decreased, in case of SPC even to BL values.
Popovtzer, 2009 [26]	PC, SCM_{ipsi}	BL 3m post-RT	Sign. decrease in T1 SI in all muscles (SPC, MPC, IPC, SCM) receiving >50 Gy. Sign. linear increase in T2 SI with dose for PC, but not SCM. T2 SI increased by 200% and 50%, respectively, in PC and SCM receiving >50 Gy. Dose-dependent thickening after therapy of PC, whereas SCM decreased in size, independent of general weight loss. Two FT-dependent patients with above average T1 SI decrease and T2 SI increase.

ADM: anterior digastric muscle, BL: baseline, FT: feeding tube, GG: genioglossus, ipsi: ipsilateral, ITM: intrinsic tongue muscle, IPC: inferior pharyngeal constrictor, m: month, MH: mylohyoid, MM: masseter, MP: medial pterygoid, MPC: medial pharyngeal constrictor, OAR: organ at risk, PC: pharyngeal constrictor, PDM: posterior digastric muscle, RT: radiotherapy, SCM: sternocleidomastoid, SI: signal intensity, sign.: significant/ly, SPC: superior pharyngeal constrictor, T1c: T1 post contrast, w: week.

after 3 months from completion of radiotherapy [26]. They analyzed the pharyngeal constrictor and the sternocleidomastoid muscle.

3.2.1. T1

No significant change could be detected for the different swallowing muscles between pre- and mid-treatment, and also not for post-treatment [11]. Furthermore, Meheissen et al. could not find a correlation between T1 SI change with dose to the muscles mid- and post-treatment [11]. Popovtzer et al. confirms this finding for the pharyngeal constrictors receiving a mean dose <50 Gy, however they could show that muscles receiving >50 Gy had a significantly lower signal intensity post-RT [26]. Messer et al. calculated a cutoff-dose of 62.25 Gy to detect changes in T1 SI pre- to

late post-treatment and could show that the superior pharyngeal constrictors (SPC) receiving more than this value had a significant decrease in T1 SI over time [15].

Post-treatment, a significant decrease in T1 SI of all muscles analyzed together was reported for the group of patients developing moderate to severe radiation-induced dysphagia [11], and a more than average decrease in T1 SI was found in the two patients with feeding tube dependency [26].

3.2.2. T2

The only muscle with a significant T2 SI increase at mid-treatment and also early post-treatment was the medial pharyngeal constrictor (MPC) [11].

A significant linear increase in T2 SI with dose has been demonstrated in the pharyngeal constrictors from pre- to post-treatment [26]. Analyzing all muscles together, a significant correlation between T2 SI change and dose could be found at both timepoints, mid-treatment (r = 0.2) and post-RT (r = 0.24) [11].

Patients developing moderate/severe RT-induced dysphagia showed a significant higher SI at mid-treatment for all swallowing muscles grouped together [11]. Similarly, the two patients in the study of Popovtzer et al. with feeding tube dependency had an increase above average in T2 SI of the pharyngeal constrictors [26].

3.2.3. T1 post contrast

A significant increase of the T1 post contrast SI could be demonstrated in the MPC and SPC mid- and post-RT [11]. Other muscles like the medial pterygoid, masseter, mylohyoid, genioglossus, intrinsic tongue, anterior digastric muscle and the posterior digastric muscle showed a significant increase at post-treatment only. Analyzed for all swallowing muscles together, a significant correlation between SI change and dose could be found at both time points, mid- (r = 0.14) and post-RT (r = 0.14).

3.2.4. Volume

A significant difference between muscle thickness of the pharyngeal constrictors receiving <50 Gy (mean + 66%) and >50 Gy (+118%) has been shown by Popovtzer et al. from pre- to post-treatment [26]. They also analyzed the ipsilateral sternocleidomastoid muscle and found a decrease in size for doses >50 Gy, but not for <50 Gy. No statistically significant correlation between weight loss and muscle thickness was found, indicating that the decrease in muscle thickness was most likely due to therapy [26].

3.2.5. Summary

To summarize, the studies could show changes most pronounced in the muscles receiving high doses, respectively in the closest swallowing muscles to the PTV, the MPC and SPC, indicating radiation-induced inflammation and edema. It remains unclear if T1, T1 post contrast or T2 SI is most predictive for outcome. During radiotherapy, changes in SI have already clinical impact but the appropriate cutoff value is still unclear, also for the dose. Further research needs to be done, with more patients included than in the above mentioned studies with all <75 patients and with more information regarding radiation doses and clinical parameters like feeding tube dependency. Furthermore, there is a great lack of functional imaging in the muscles of the head and neck region. Nevertheless, because of time-consuming delineation, an implementation into clinical use seems only to be feasible when using a proper auto-contouring tool for all the muscles or focusing on the muscles most adjacent to the high-dose areas only.

Table 9
Radiation-induced MR changes in bony structures of the head and neck region measured with T1, T2 and DCE.

Author, year	OAR	Time point	Main findings
Hatakeyama, 2017 [14]	Hyoid	BL Median 6m post-RT	Post-RT, the hyoid bone of 27 patients (69%) remained T1 hyperintense and T2 hypointense. 12 patients developed T1 hypointensity, of which 9 (23%) were categorized as having inflammation (T2 hyperintense) and 3 (8%) as fibrosis (T2 hypointense).
Sandulache, 2016 [16]	Mandible	BL 3-4w after RT-start 6-8w post-RT	58%/43% of patients with increase in k_{trans} (+12.5 min^{-1}/+7.5 min^{-1}), 39%/37% with decrease (−3.8 min^{-1}/−4.2 min^{-1}), 3%/20% stable at mid- and post-RT, respectively. 68%/70% with increase in v_e (+5.0/+15.5), 19%/17% with decrease (−3.6/−1.7) mid- and post-RT, respectively. Consistency between k_{trans} and v_e in 65%/50% of patients mid- and post-RT, respectively. One patient with ORN showed k_{trans} and v_e increase mid-RT and a decrease of both parameters post-RT.

BL: baseline, k_{trans}: volume transfer coefficient, m: month, OAR: organ at risk, ORN: osteoradionecrosis, RT: radiotherapy, v_e: extravascular volume fraction w: week.

Table 10
Overview of factors influencing study quality and inter-study-comparison.

Confounding factors	Effect on	Relevance for	Possible problem solution
Patient selection	Image parameters	Comparison between different studies	Strict inclusion criteria or large study cohort
MRI machine, vendor	Inter-vendor reproducibility	Patients changing the MR machine for follow-up scan Comparison between different studies	More comparison studies using different MRI machines
MRI machine, field strength	SNR Susceptibility artifacts at boundaries	Delineation/analysis esp. of structures near boundaries	Using/developing further artifact reduction methods Spin echo instead of GRE, short TE
RF coils, shape/channels	Image quality (spatial resolution, SNR)	Delineation	Coils shaped for use with RT immobilization
Immobilization	Motion-related artifacts Positional reproducibly	Delineation Rigid image registration of structures contoured on other sequences	Use of immobilization devices (Mask/Bite block/Dental Stent) for imaging
Image acquisition parameters	Image parameters Scan-rescan repeatability	Patients changing the MR machine for follow-up scan Comparison between different studies	Use of standardized image acquisition parameters/QIBA guideline for head and neck
Segmentation	Image parameters NTCP	Generalization of study outcomes	Use of contouring guidelines
Post-processing method	Image parameters	Comparison between different studies	Use of standardized computer programs
Statistical analysis	Statistical output	Comparison between different studies	Less influence if delta change is used

GRE: gradient echo, QIBA: Quantitative Imaging Biomarkers Alliance, NTCP: normal tissue complication probability, RF: radiofrequency, SNR: signal-to-noise ratio, TE: echo time.

3.3. Quantitative changes in MRI of the bony structures in the head and neck region (Table 9)

Only two studies analyzed the effect of radiotherapy on MR changes in bones of the head and neck region, one with an additional measurement during radiotherapy and one with pre- and post-RT scans only (Table 9). Especially the first one [16] appears more like a kind of feasibility study to investigate if there is at all a change in DCE imaging parameters of the mandible caused by radiotherapy.

3.3.1. T1/T2

The normal appearance of the hyoid bone, defined as T1 hyper- and T2 hypointense, remained unchanged after radiotherapy in 69% of the OPC patients [14]. However, 23% of the patients developed inflammation, defined as T1 hypointensity and T2 hyperintensity and 8% signs of RT-induced fibrosis (T1 and T2 hypointensity) [14].

3.3.2. DCE

A predominant increase in k_{trans} could be shown in 58% and 43% and in v_e in 68% and 70% of patients at mid- and post-RT, respectively [16]. 65% of the patients showed a correlation between the dose-dependent trend in k_{trans} and v_e. Only one patient of the cohort developed osteoradionecrosis (ORN) with decreased imaging parameters [16].

3.3.3. Summary

Preliminary findings suggest T1 hypointensity and decreased DCE parameters as indicator for ORN. More studies have to be conducted with larger patient cohorts and longer follow-up, as severe ORN is a rare finding and occurs approximately after a median of 8 months post-RT [6]. Furthermore, more patient details like prior dental procedures and the use of fluoride prophylaxis should be included and a more accurate, voxel-by-voxel dose-toxicity comparison performed.

A promising, ongoing study with endpoint ORN (NCT03145077), is currently conducting repetitive MRIs already in patients without apparent ORN, to find early changes in the bone before ORN becomes clinically symptomatic.

3.4. Limitations (Fig. 1, Table 10)

Comparability of the different studies is hampered by factors like the use of different MR scanners [29,30] with 1.5 or 3.0 Tesla field strength and variable image acquisition parameters [29–31], like different b-values, slice thickness, slice gap, TR/TE (repetition time/echo time). It has also to be taken into account that different coils influence the image quality [32,33] and only in a few cases, RT-immobilization devices, which have an effect on positional stability [34] have been used for MR imaging.

The different post-processing methods applied in these studies can also affect the imaging parameters by use of different software for calculation or the use of automatically generated maps [35].

Different segmentation methods for the region of interest (ROI) have been used across the studies as some contoured the whole parotid gland, whereas others only focused on three slices with the largest area of parotid gland. Some delineated the gland on all MR sequences, whereas others only contoured on T1 or T2 and used rigid or deformable registration to copy the ROIs to other sequences or used auto-contouring and adapted the contours afterwards. Furthermore, larger vessels and ducts were not excluded from the parotid glands in all studies. The influence of such inconsistencies has been shown to affect the mean dose to the structures as well as the normal tissue complication probabilities (NTCP) [36].

Patient numbers are low in all of the published studies and even with a mix of intensity modulated photon and proton therapy in three studies.

For future comparison of MR studies across different institutes or for homogenization in multi-institutional trials it is crucial to achieve more generalizable results. To achieve this, standardization of the image acquisition (MRI machines, radiofrequency coils, imaging protocols), as well as the patient setup and for DCE imaging the Gadolinium injection parameters (dose of contrast agent, timing of imaging, use of individual or population-derived arterial input function, etc.), is urgently needed.

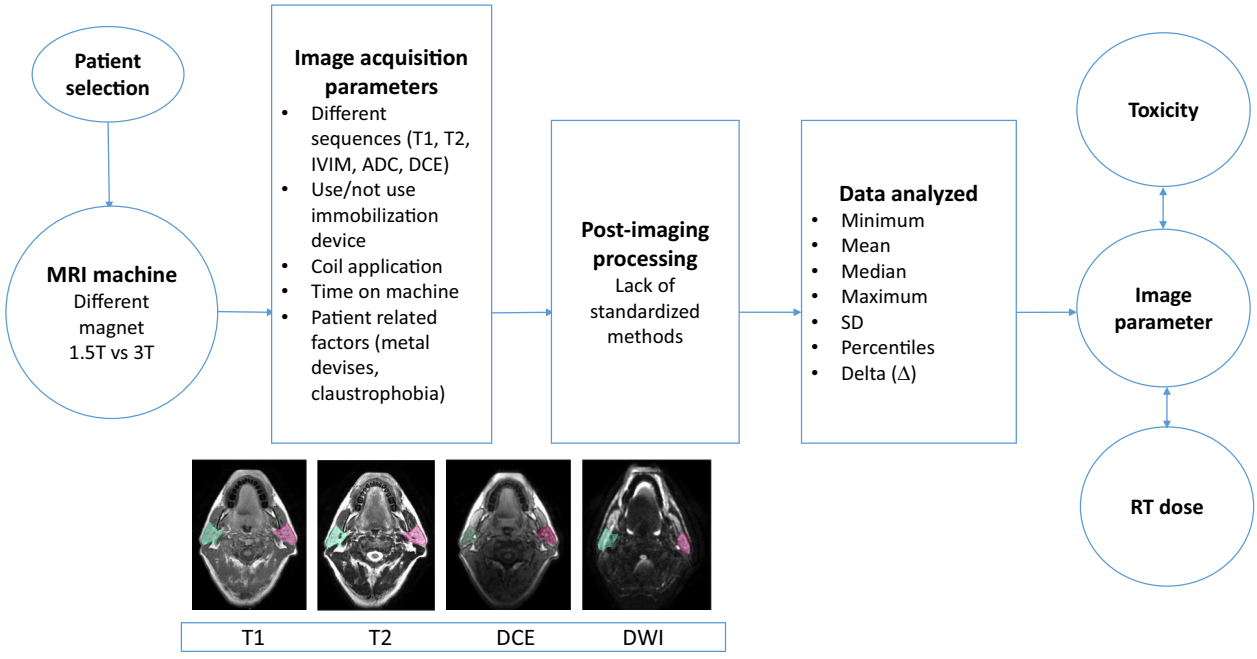

Fig. 1. Variables from patient selection to data analysis, influencing imaging parameters and the correlation with toxicity measurements and radiotherapy dose. ADC: apparent diffusion coefficient, DCE: dynamic contrast enhanced, IVIM: intravoxel incoherent motion imaging, RT: radiotherapy, SD: standard deviation, T: Tesla.

4. Conclusion

This review gives a comprehensive overview of MR changes through the course of radiotherapy reported by different studies. Consistently, a decrease in salivary gland volume, duct visibility and an increase in T2 SI, v_e and ADC was reported. So far, the conducted studies have included only low patient numbers of up to 72 patients (median: 21 patients). Further research on larger patient cohorts is strongly warranted to confirm the preliminary findings.

5. Declarations of interest

None.

Funding source

Sonja Stieb is funded by the Swiss Cancer League (BIL KLS-4300-08-2017). Baher Elgohari is funded by the Egyptian Cultural and Educational bureau. Clifton D. Fuller received funding from the National Institute for Dental and Craniofacial Research Award (1R01DE025248-01/R56DE025248) and Academic-Industrial Partnership Award (R01 DE028290), the National Science Foundation, USA (NSF), Division of Mathematical Sciences, Joint NIH/NSF Initiative on Quantitative Approaches to Biomedical Big Data (QuBBD) Grant (NSF 1557679), the NIH Big Data to Knowledge (BD2K) Program of the National Cancer Institute (NCI) Early Stage Development of Technologies in Biomedical Computing, Informatics, and Big Data Science Award (1R01CA214825), the NCI Early Phase Clinical Trials in Imaging and Image-Guided Interventions Program (1R01CA218148), the NIH/NCI Cancer Center Support Grant (CCSG) Pilot Research Program Award from the UT MD Anderson CCSG Radiation Oncology and Cancer Imaging Program (P30CA016672), the NIH/NCI Head and Neck Specialized Programs of Research Excellence (SPORE) Developmental Research Program Award (P50 CA097007) and the National Institute of Biomedical Imaging and Bioengineering (NIBIB) Research Education Program (R25EB025787). Dr. Fuller has received direct industry grant support, speaking honoraria and travel funding from Elekta AB.

References

[1] Gillison ML et al. Radiotherapy plus cetuximab or cisplatin in human papillomavirus-positive oropharyngeal cancer (NRG Oncology RTOG 1016): a randomised, multicentre, non-inferiority trial. Lancet 2019;393(10166):40–50.
[2] O'Sullivan B et al. Development and validation of a staging system for HPV-related oropharyngeal cancer by the International Collaboration on Oropharyngeal cancer Network for Staging (ICON-S): a multicentre cohort study. Lancet Oncol 2016;17(4):440–51.
[3] Mirghani H, Blanchard P. Treatment de-escalation for HPV-driven oropharyngeal cancer: where do we stand? Clin Transl Radiat Oncol 2018;8:4–11.
[4] Deshpande TS et al. Radiation-related alterations of taste function in patients with head and neck cancer: a systematic review. Curr Treat Options Oncol 2018;19(12):72.
[5] Dornfeld K et al. Radiation doses to structures within and adjacent to the larynx are correlated with long-term diet- and speech-related quality of life. Int J Radiat Oncol Biol Phys 2007;68(3):750–7.
[6] Peterson DE et al. Osteoradionecrosis in cancer patients: the evidence base for treatment-dependent frequency, current management strategies, and future studies. Support Care Cancer 2010;18(8):1089–98.
[7] Martens RM et al. Functional imaging early during (chemo)radiotherapy for response prediction in head and neck squamous cell carcinoma; a systematic review. Oral Oncol 2019;88:75–83.
[8] Marzi S et al. Radiation-induced parotid changes in oropharyngeal cancer patients: the role of early functional imaging and patient−/treatment-related factors. Radiat Oncol 2018;13(1).
[9] Zhou N et al. Early evaluation of radiation-induced parotid damage in patients with nasopharyngeal carcinoma by T2 mapping and mDIXON Quant imaging: initial findings. Radiat Oncol 2018;13(1):22.
[10] Zhang Q et al. Early changes in apparent diffusion coefficient for salivary glands during radiotherapy for nasopharyngeal carcinoma associated with xerostomia. Korean J Radiol 2018;19(2):328–33.
[11] Joint H, Neck Radiotherapy MRIDC. A prospective longitudinal assessment of MRI signal intensity kinetics of non-target muscles in patients with advanced stage oropharyngeal cancer in relationship to radiotherapy dose and post-treatment radiation-associated dysphagia: preliminary findings from a randomized trial. Radiother Oncol 2019;130:46–55.
[12] Zhou N et al. Early changes of irradiated parotid glands evaluated by t1rho-weighted imaging: a pilot study. J Comput Assist Tomogr 2017;41(3):472–6.
[13] Loimu V et al. Diffusion-weighted magnetic resonance imaging for evaluation of salivary gland function in head and neck cancer patients treated with intensity-modulated radiotherapy. Radiother Oncol 2017;122(2):178–84.
[14] Hatakeyama H et al. Osteoradionecrosis of the hyoid bone after intra-arterial chemoradiotherapy for oropharyngeal cancer: MR imaging findings. Cancer Imaging 2017;17(1):22.
[15] Messer JA et al. Magnetic resonance imaging of swallowing-related structures in nasopharyngeal carcinoma patients receiving IMRT: longitudinal dose-response characterization of quantitative signal kinetics. Radiother Oncol 2016;118(2):315–22.
[16] Joint H, Neck Radiotherapy MRIDC. Dynamic contrast-enhanced MRI detects acute radiotherapy-induced alterations in mandibular microvasculature: prospective assessment of imaging biomarkers of normal tissue injury. Sci Rep 2016;6:29864.
[17] Marzi S et al. Early radiation-induced changes evaluated by intravoxel incoherent motion in the major salivary glands. J Magn Reson Imaging 2015;41(4):974–82.
[18] Juan CJ et al. Temporal evolution of parotid volume and parotid apparent diffusion coefficient in nasopharyngeal carcinoma patients treated by intensity-modulated radiotherapy investigated by magnetic resonance imaging: a pilot study. PLoS One 2015;10(8):e0137073.
[19] Doornaert P et al. Use of diffusion-weighted magnetic resonance imaging (DW-MRI) to investigate the effect of chemoradiotherapy on the salivary glands. Acta Oncol 2015;54(7):1068–71.
[20] Zhang Y et al. Diffusion-weighted MR imaging of salivary glands with gustatory stimulation: comparison before and after radiotherapy. Acta Radiol 2013;54(8):928–33.
[21] Ou D et al. Magnetic resonance sialography for investigating major salivary gland duct system after intensity-modulated radiotherapy of nasopharyngeal carcinoma. Int J Clin Oncol 2013;18(5):801–7.
[22] Cheng CC et al. Parotid perfusion in nasopharyngeal carcinoma patients in early-to-intermediate stage after low-dose intensity-modulated radiotherapy: evaluated by fat-saturated dynamic contrast-enhanced magnetic resonance imaging. Magn Reson Imaging 2013;31(8):1278–84.
[23] Houweling AC et al. MRI to quantify early radiation-induced changes in the salivary glands. Radiother Oncol 2011;100(3):386–9.
[24] Lee FK et al. Radiation injury of the parotid glands during treatment for head and neck cancer: assessment using dynamic contrast-enhanced MR imaging. Radiat Res 2011;175(3):291–6.
[25] Kan T et al. Radiation-induced damage to microstructure of parotid gland: evaluation using high-resolution magnetic resonance imaging. Int J Radiat Oncol Biol Phys 2010;77(4):1030–8.
[26] Popovtzer A et al. Anatomical changes in the pharyngeal constrictors after chemo-irradiation of head and neck cancer and their dose-effect relationships: MRI-based study. Radiother Oncol 2009;93(3):510–5.
[27] Dirix P et al. Diffusion-weighted magnetic resonance imaging to evaluate major salivary gland function before and after radiotherapy. Int J Radiat Oncol*Biol*Phys 2008;71(5):1365–71.
[28] Astreinidou E et al. 3D MR sialography as a tool to investigate radiation-induced xerostomia: feasibility study. Int J Radiat Oncol*Biol*Phys 2007;68(5):1310–9.
[29] Zhou X et al. Scan-rescan repeatability and cross-scanner comparability of DTI metrics in healthy subjects in the SPRINT-MS multicenter trial. Magn Reson Imaging 2018;53:105–11.
[30] Lee Y et al. Establishing intra- and inter-vendor reproducibility of T1 relaxation time measurements with 3T MRI. Magn Reson Med 2019;81(1):454–65.
[31] Becker AS et al. Diffusion-weighted imaging of the abdomen: Impact of b-values on texture analysis features. NMR Biomed 2017;30(1).
[32] Parikh PT et al. Evaluation of image quality of a 32-channel versus a 12-channel head coil at 1.5T for MR imaging of the brain. AJNR Am J Neuroradiol 2011;32(2):365–73.
[33] McGee KP et al. Characterization and evaluation of a flexible MRI receive coil array for radiation therapy MR treatment planning using highly decoupled RF circuits. Phys Med Biol 2018;63(8):p. 08NT02.
[34] Ding Y et al. Prospective observer and software-based assessment of magnetic resonance imaging quality in head and neck cancer: should standard positioning and immobilization be required for radiation therapy applications? Pract Radiat Oncol 2015;5(4):e299–308.
[35] Zeilinger MG et al. Impact of post-processing methods on apparent diffusion coefficient values. Eur Radiol 2017;27(3):946–55.
[36] Brouwer CL et al. Differences in delineation guidelines for head and neck cancer result in inconsistent reported dose and corresponding NTCP. Radiother Oncol 2014;111(1):148–52.